nature methods

SUPPLEMENTARY INFORMATION

https://doi.org/10.1038/s41592-019-0539-z

In the format provided by the authors and unedited.

Robust and automated detection of subcellular morphological motifs in 3D microscopy images

Meghan K. Driscoll[1,2], Erik S. Welf[1,2], Andrew R. Jamieson[1,2], Kevin M. Dean[1,2], Tadamoto Isogai[1,2], Reto Fiolka[1,2] and Gaudenz Danuser[1,2]*

[1]Lyda Hill Department of Bioinformatics, University of Texas Southwestern Medical Center, Dallas, TX, USA. [2]Department of Cell Biology, University of Texas Southwestern Medical Center, Dallas, TX, USA. *e-mail: Gaudenz.Danuser@UTSouthwestern.edu

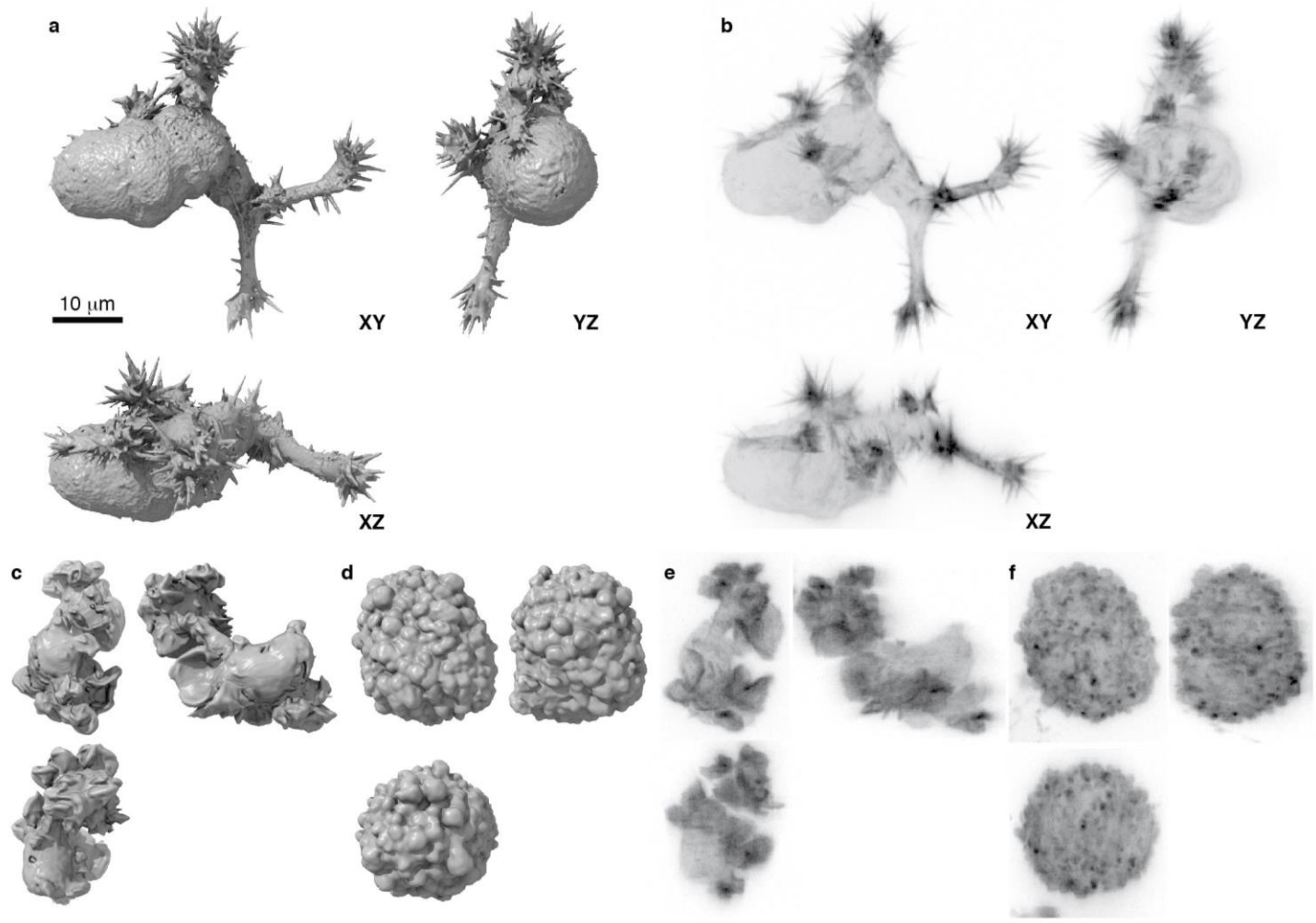

Supplementary Figure 1

More views of the cells shown in Figure 1a-f.

(**a**) Surface renderings of an HBEC expressing tractin-GFP. (**b**) MIPs of the cell shown in a. (**c**) Surface renderings of a dendritic cell expressing Lifeact-GFP. (**d**) Surface renderings of an MV3 melanoma cell expressing tractin-GFP. (**e**) MIPs of the cell shown in c. (**f**) MIPs of the cell shown in d.

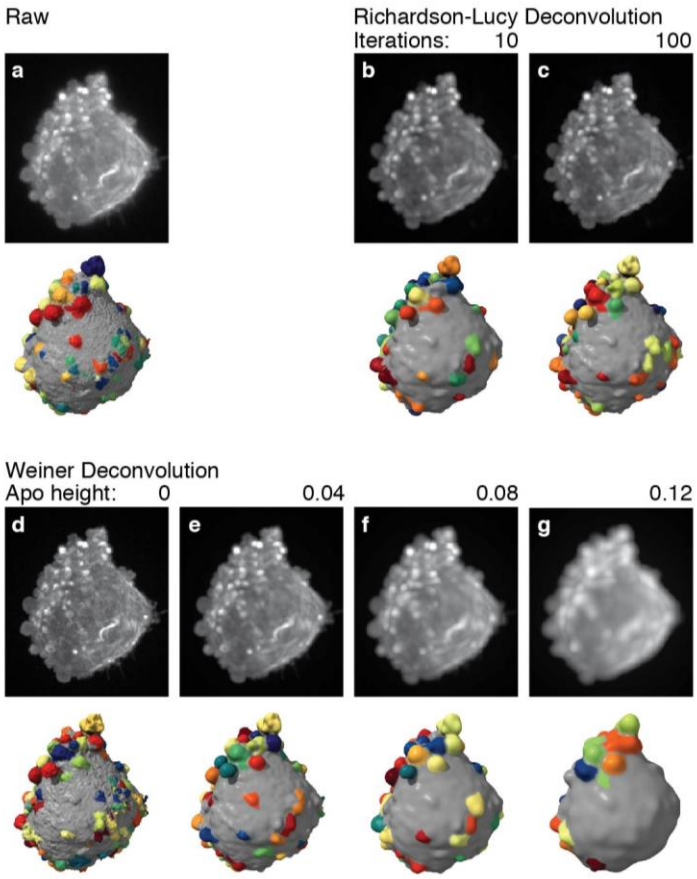

Supplementary Figure 2

Variations in parameters governing deconvolution.

For the cell shown in Figure 2f-p, a MIP (top) and the corresponding rendered surface colored by bleb detection (bottom) are shown. The blebs were detected using an SVM model derived from Weiner deconvolved images with an apodization height of 0.04. Images are (**a**) not deconvolved, Richardson-Lucy deconvolved for (**b**) 10 iterations and (**c**) 100 iterations, and Weiner deconvolved with an apodization height of (**d**) 0.00, (**e**) 0.04, (**f**) 0.08, (**g**) and 0.12.

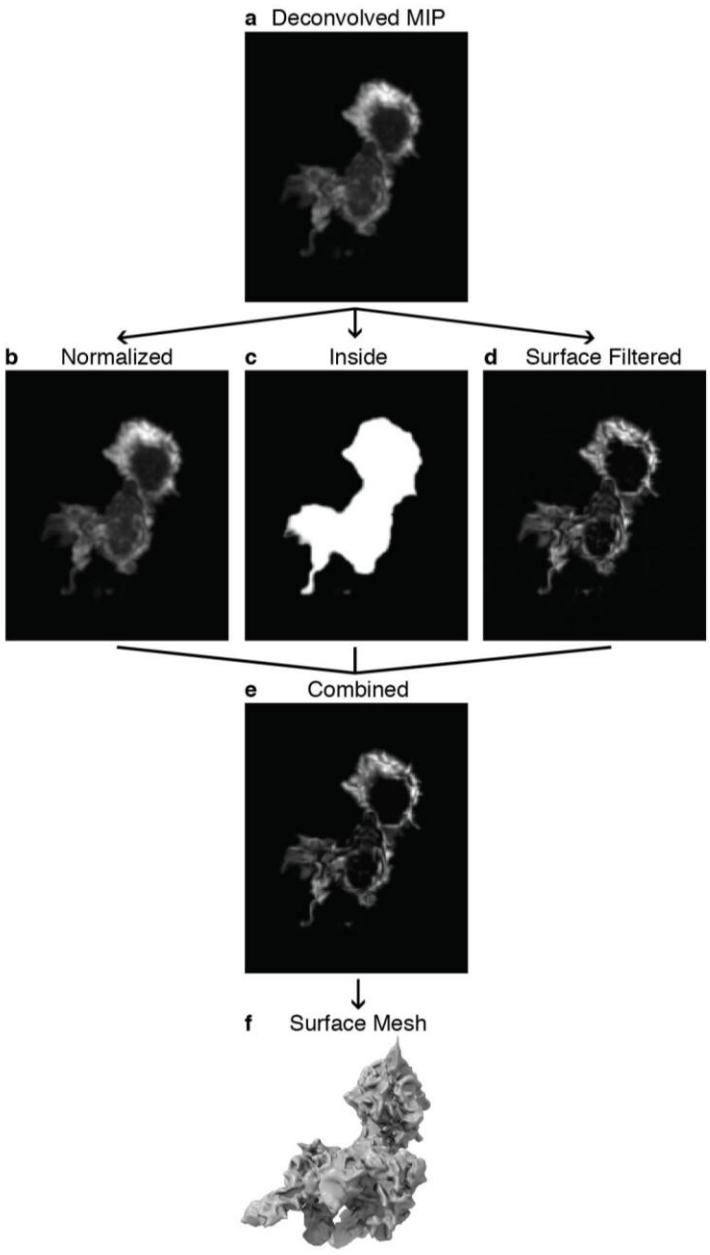

Supplementary Figure 3

Segmentation of dendritic cells.

(**a**) A MIP across 4 µm of a deconvolved image of a dendritic cell expressing LifeAct-GFP. This image was segmented by processing the deconvolved image into three images that accentuate different features: (**b**) a renormalized deconvolved image, (**c**) an image that emphasizes the interior of the cell, and (**d**) an image that emphasizes planar features, such as lamellipodia. These three images were combined into (**e**) a composite image. (**f**) Finally, a mesh was generated from an isosurface of the composite image.

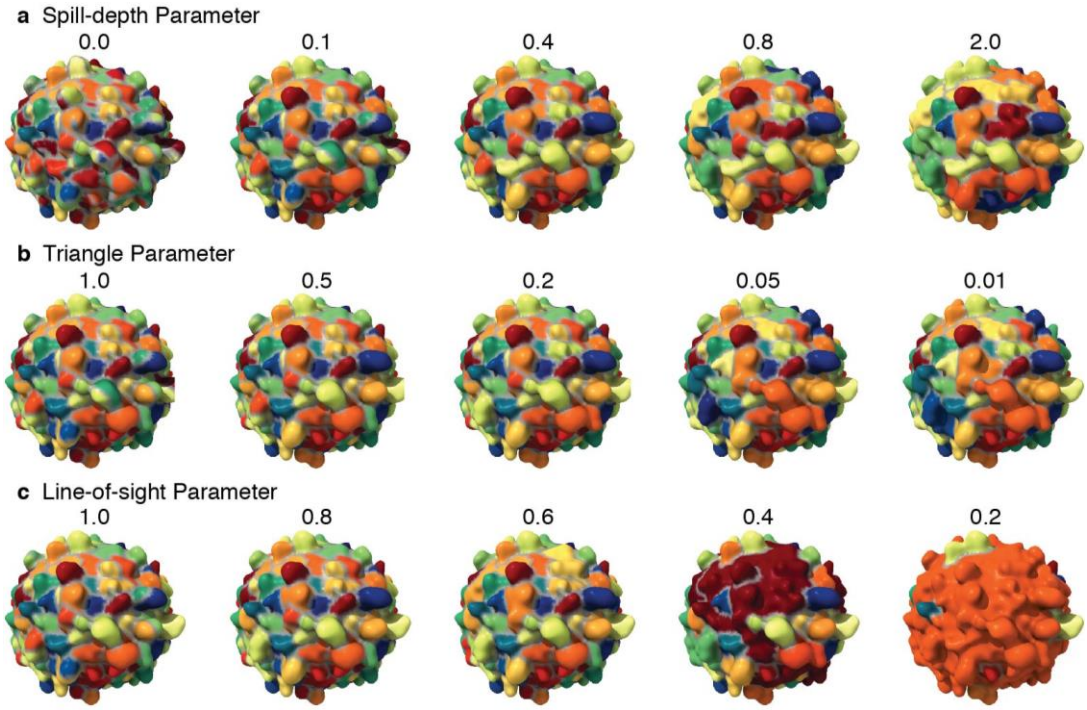

Supplementary Figure 4

Variations in parameters governing patch merging.

(**a**) Spill-depth based merging without triangle or line-of-sight (LOS) merging. A spill-depth ratio of 0.15 is used throughout the paper. (**b**) Triangle merging following spill-depth merging but without LOS merging. Elsewhere in the paper a triangle parameter of 0.7 is used. (**c**) LOS merging following spill-depth merging but without triangle merging. Elsewhere in the paper an LOS parameter of 0.7 is used.

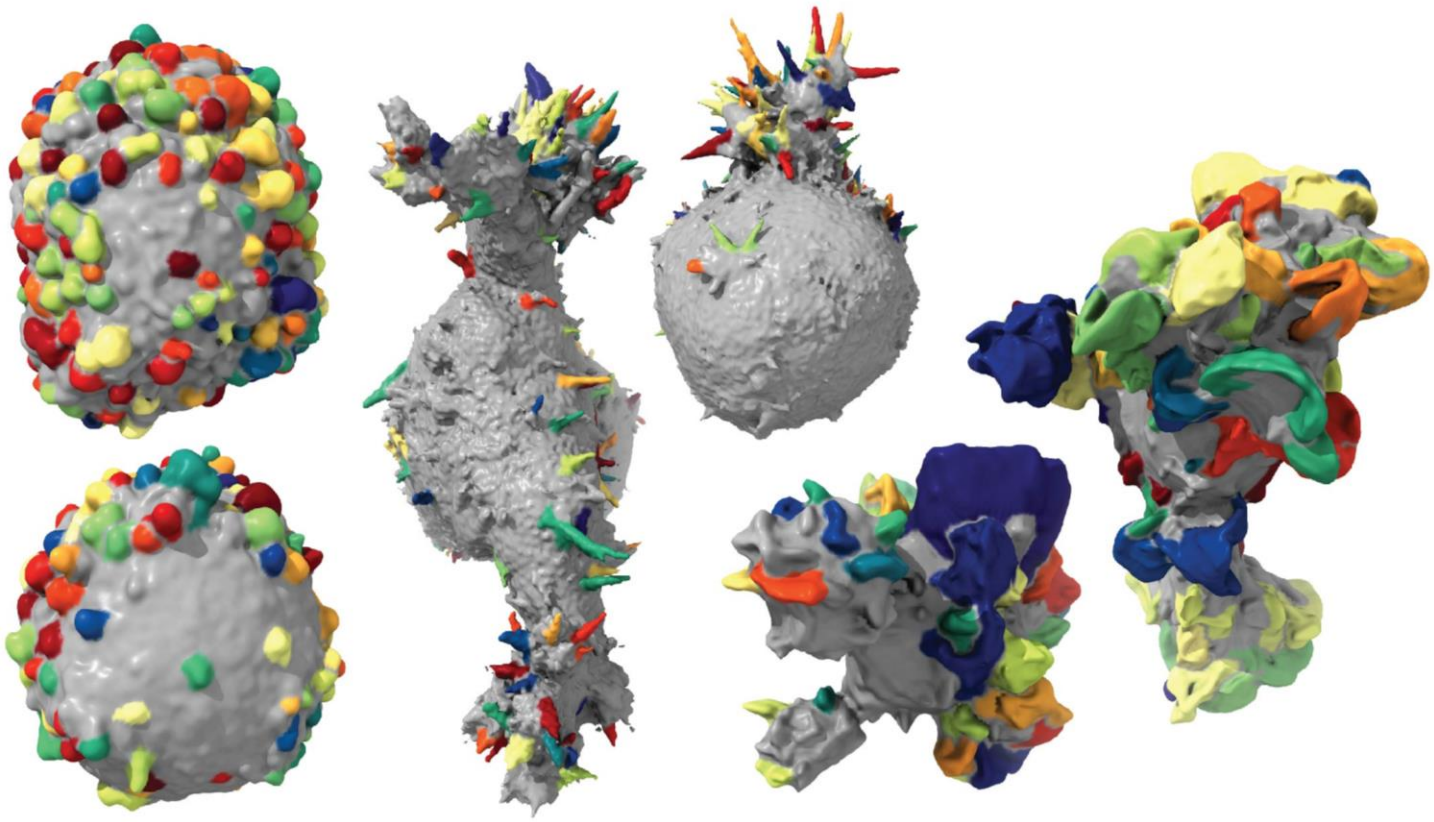

Supplementary Figure 5

Additional example morphological motif detections.

Blebs are detected on two melanoma cells (left), filopodia on two HBEC cells (center) and lamellipodia on two dendritic cells (right).

a

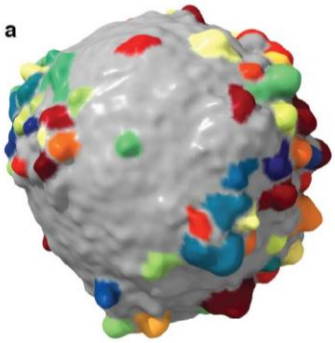

b	Click on blebs	Click on not blebs	Click on certain
True positives	101/279	132/279	20/39
True negatives	127/279	100/279	19/39
False positives	42/279	11/279	0/39
False negatives	9/279	36/279	0/39
Precision	0.71	0.92	1.0
Recall	0.92	0.79	1.0
F1 score	0.80	0.85	1.0
% clicked on	0.39	0.40	0.14

c Number of cells trained on (individual trainer):

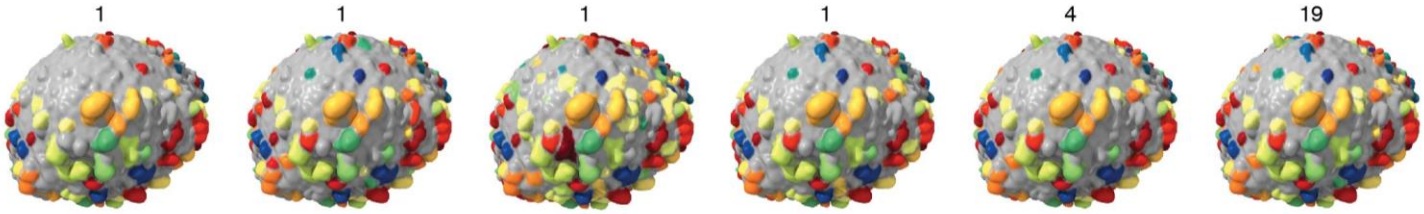

d Three different trainers (training on the same four cells):

Supplementary Figure 6

Validation of diverse bleb models.

(**a**) A melanoma cell with blebs detected via a model trained by a single user who clicked on patches that were certainly blebs or certainly not blebs. (**b**) Validation metrics for models trained by the same user on three different cells and applied to the cell shown in a. For the “Click on blebs” column, training data was generated by asking the user to click on all patches that are blebs. For the “Click on not blebs” column, the user was asked to click on all patches that are not blebs. Finally, for the “Click on certain” column, the user was asked to click on all patches that are certainly blebs and then asked to click on all patches that are certainly not blebs. For this column, the user clicked on 39 of the 279 patches. (**c**) Models trained by the same user on four distinct MV3 cells (left), on those four cells combined (center), and on 19 MV3 cells (right). (**d**) Models trained by three different users on the same four MV3 cells as in c.

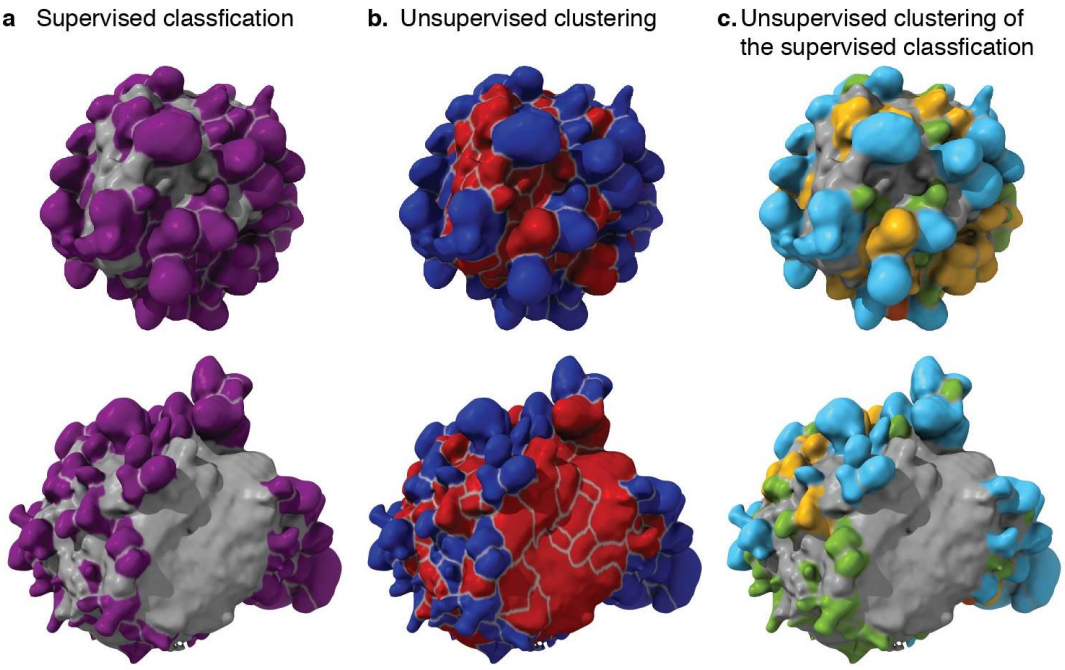

Supplementary Figure 7

Unsupervised clustering of patches and motifs.

(**a**) Supervised, SVM-based classification of patches into blebs (purple) and not blebs (gray). The SVM was trained on seven MV3 cells imaged via ASLM. (**b**) For the same set of cells, an unsupervised hierarchical clustering of patches into 2 clusters. (**c**) Unsupervised hierarchical clustering into 4 clusters of the supervised classification shown in a.

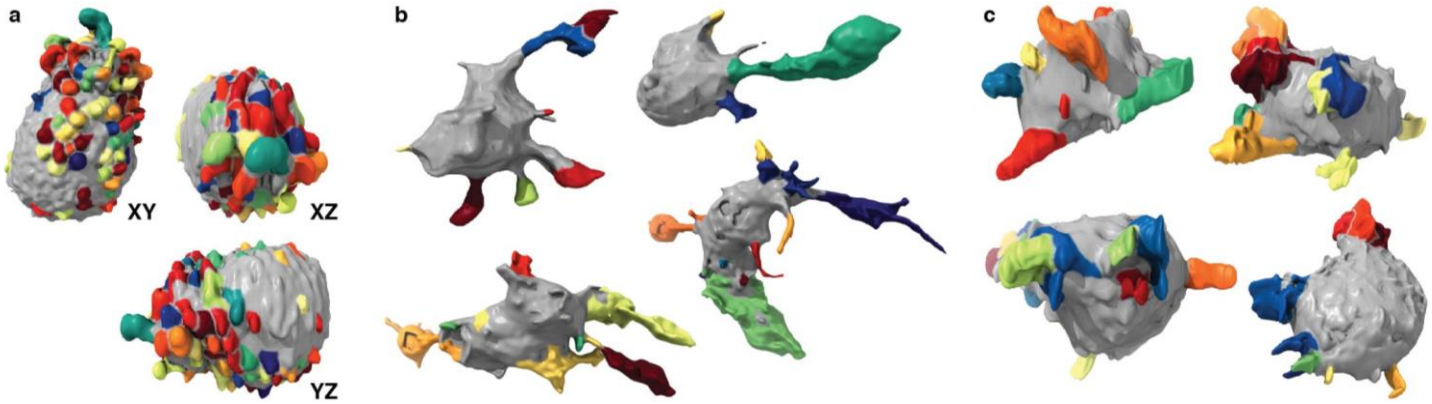

Supplementary Figure 8

Additional example morphological motif detections of cells imaged via diverse microscopy modalities.

(**a**) Three views of blebs detection on an MV3 cell expressing tractin-GFP imaged via a laser scanning confocal microscope. The bleb detection model was trained on eight MV3 cells imaged via the same microscope. (**b**) Extensions detected on microglia cells imaged within a zebrafish via a Zeiss LightSheet Z.1 light-sheet microscope. The extension detection model was trained on eight such cells. (**c**) Lamellipodia detected on a T cell imaged via lattice light-sheet microscopy. The lamellipodia detection model was trained on thirteen dendritic cells imaged via meSPIM.

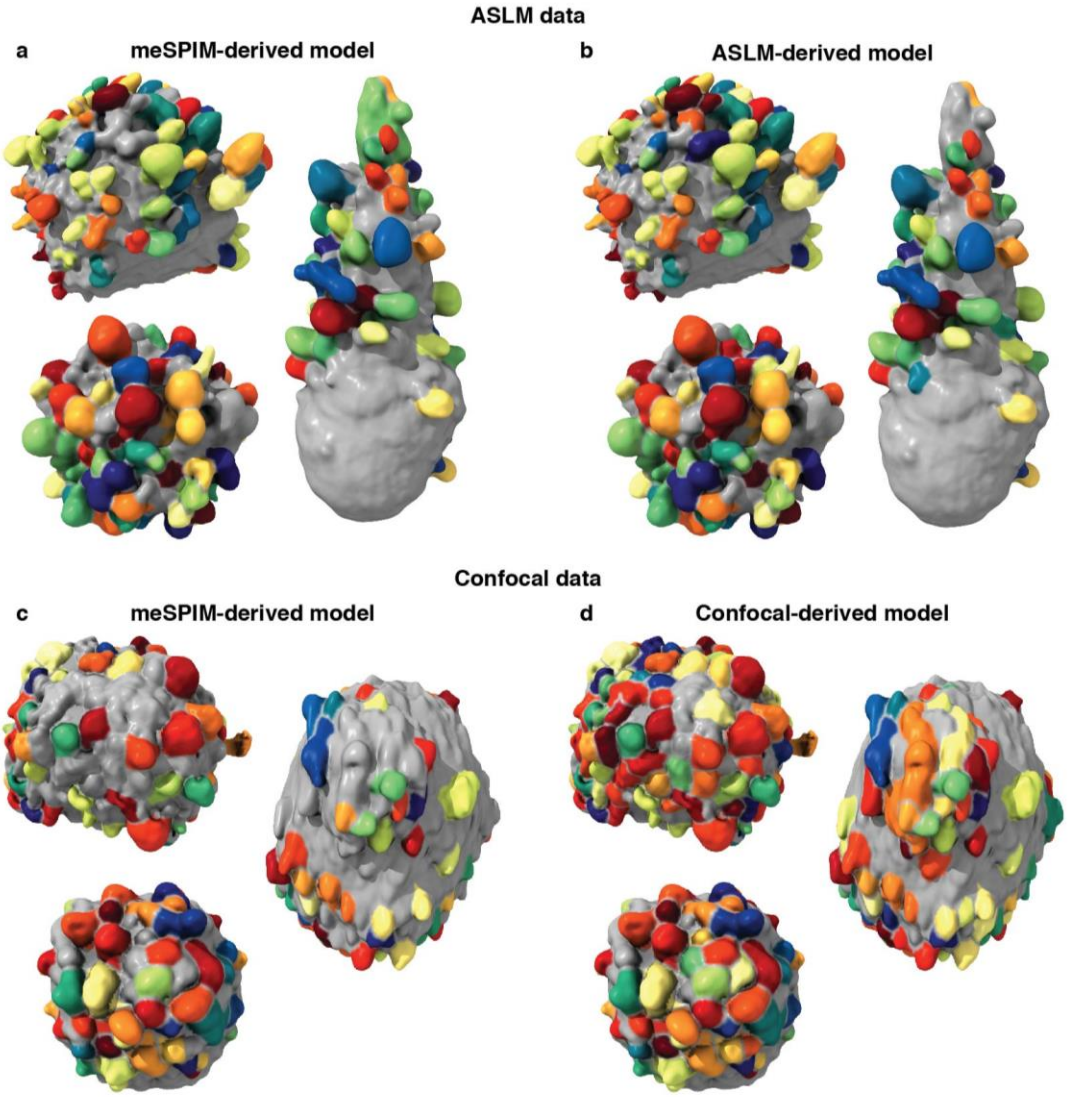

e

Model	Data	Precision	Recall	F_1
meSPIM	meSPIM	98.1	99.2	98.7
ASLM	ASLM	96.3	96.3	96.3
meSPIM	ASLM	98.4	94.3	96.3
confocal	confocal	95.5	93.4	94.4
meSPIM	confocal	95.7	80	87.2

Supplementary Figure 9

Workflow validation on confocal and ASLM acquired images.

MV3 cells expressing cytosolic GFP imaged via ASLM, a high-resolution light-sheet imaging modality, with blebs detected by a model trained on (**a**) nineteen MV3 cells expressing tractin-GFP imaged via meSPIM and (**b**) eight cells expressing cytosolic GFP imaged via ASLM. MV3 cells expressing tractin-GFP imaged via a laser scanning confocal microscope with blebs detected by a model trained on (**c**) nineteen MV3 cells expressing tractin-GFP imaged via meSPIM and (**d**) eight cells expressing tractin-GFP imaged via a confocal microscope. (**e**) Validation of bleb detection models trained on MV3 melanoma cells imaged via diverse microscopes (model column) and applied to the same or different sets of MV3 melanoma cell images (data column).

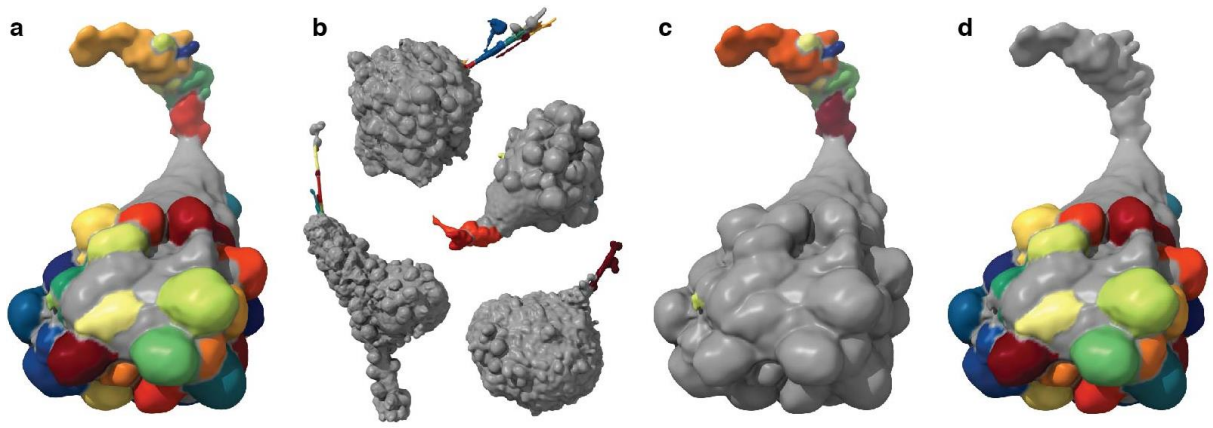

Supplementary Figure 10

Uropod and retraction fiber detection.

(**a**) Blebs detected on the MV3 cell shown in Fig. 6b, which is expressing GFP-Kras^{V12}, using a model trained on MV3 cells expressing tractin-GFP. Each bleb is randomly colored. (**b**) Uropods and retraction fibers detected on MV3 cells expressing GFP-Kras^{V12}. (**c**) The uropod detected on the cell shown in a. (**d**) For the same cell, detected blebs (see a) with the detected uropod patches (see c) removed.

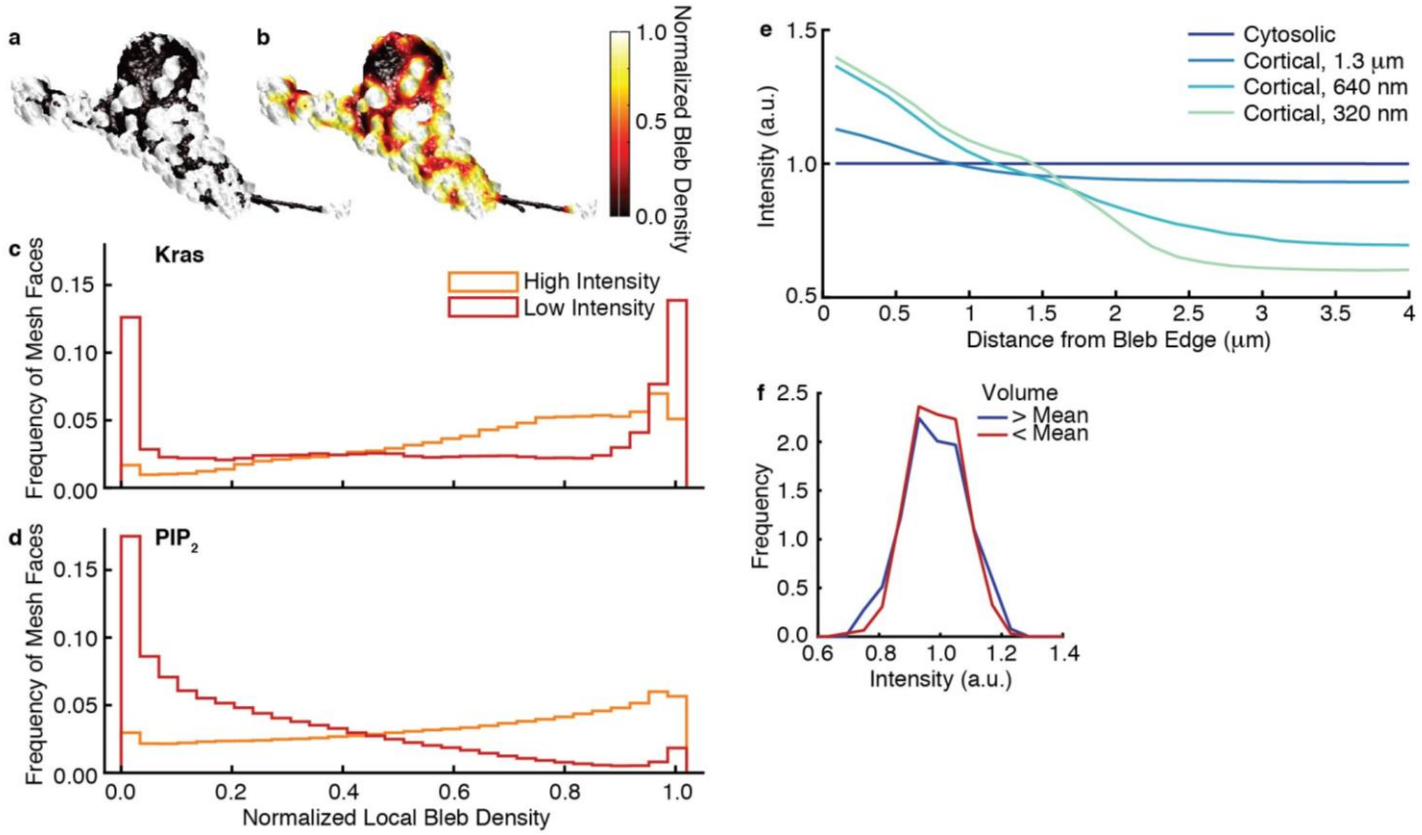

Supplementary Figure 11

Measuring intensity surface localization.

(**a**) A surface rendering of an MV3 melanoma cell with detected blebs shown white and detected non-blebs shown black. (**b**) A surface rendering of the same cell colored by normalized local bleb density. White indicates regions of high local bleb density, whereas black indicates regions of low local bleb density. Distributions of normalized bleb density for cells expressing (**c**) GFP-Kras^{V12} (n=13 cells) and (**d**) PLCΔ-PH-GFP (n=6 cells), a PIP_2 translocation biosensor. The red lines show the distribution above one standard deviation above the mean intensity, and the orange lines shows the distribution below one standard deviation below the mean intensity. (**e**) Fluorescence intensity at mesh faces vs. distance from a bleb edge for synthetic images. The dark blue line shows the intensity for 9 cytosolically labeled cells, and the lighter blue lines show the intensity for the same set of 9 cells with cortical, rather than cytosolic, labeling of various thicknesses. (**f**) Distributions of fluorescence intensity, measured over 1 μm, for 5 GFP cytosolically labeled MV3 cells. The solid line shows the intensity distribution for mesh faces on blebs, whereas the dashed line shows the distribution off blebs. The blue line shows the distribution for mesh faces on blebs with greater than mean bleb volume, whereas the red line shows the distribution on blebs with less than mean volume.

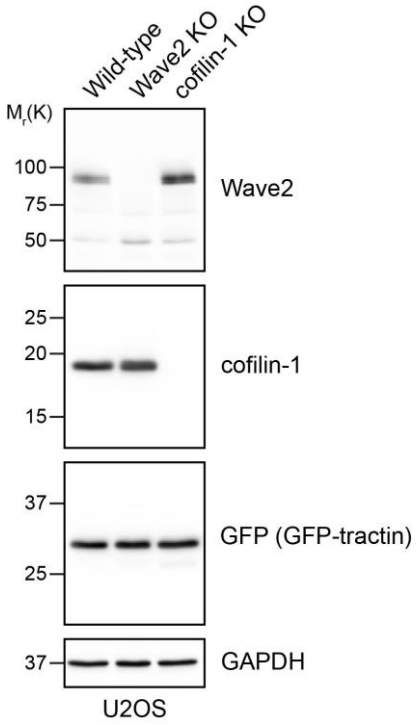

Supplementary Figure 12

Characterization of Wave2 and cofilin-1 knockout cells.

Total cell lysates (20 µg) of U2OS wild-type, Wave2 and cofilin-1 knockout cells were separated by SDS-PAGE and immunoblotted as indicated. GAPDH served as loading control. This blot is representative of two blots (n=2).

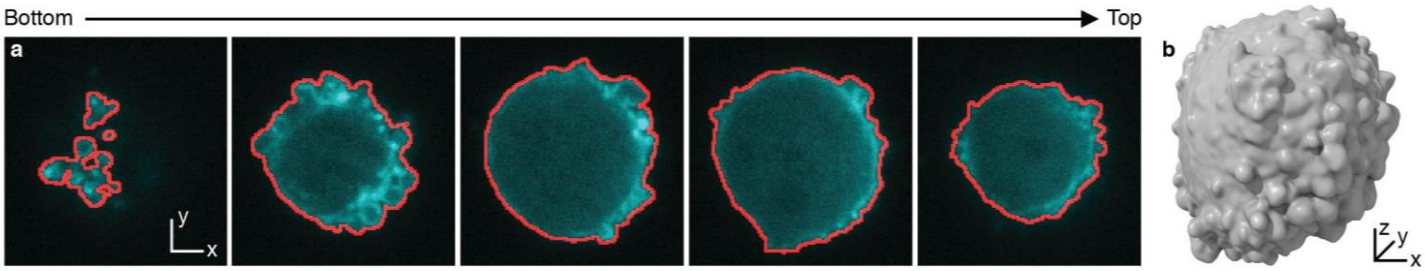

Supplementary Figure 13

Segmentation assessment.

An MV3 melanoma cell expressing tractin-GFP. (**a**) Five xy-slices sampled 4 µm apart. The raw data is shown cyan, whereas a pixelation of the mesh representing the cell surface is shown red. (**b**) A 3D rendering of the extracted cell surface for the same cell.

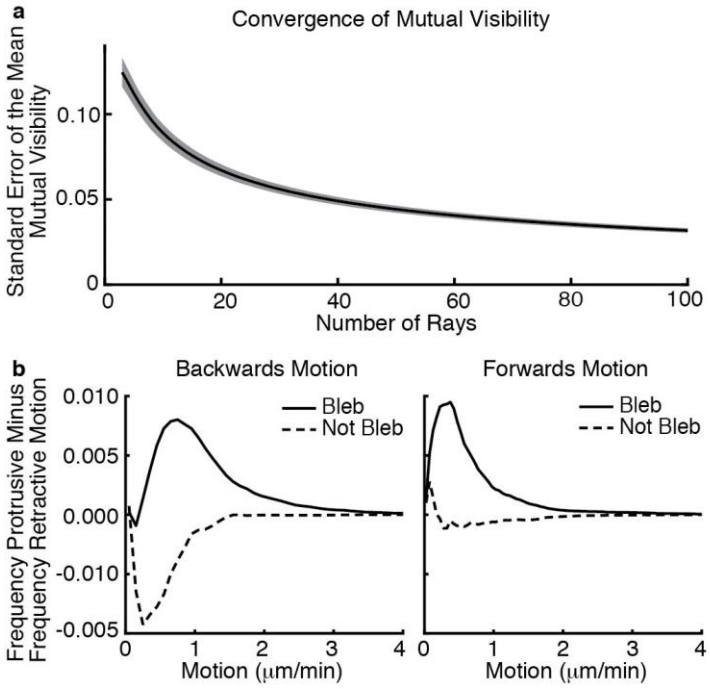

Supplementary Figure 14

Mutual visibility and motion.

(**a**) The convergence of the mutual visibility between patches as a function of number of rays tested. The black line shows the standard error about the mean mutual visibility, and the gray region shows the standard deviation of that standard error. Throughout the paper 20 rays are used to calculate mutual visibility. (**b**) The frequency of protrusive motion minus the frequency of retractive motion at mesh faces on and off blebs as a function of surface speed. The “backwards” motion algorithm, used elsewhere in the paper, is shown on the left, and the “forwards” motion algorithm is shown on the right.

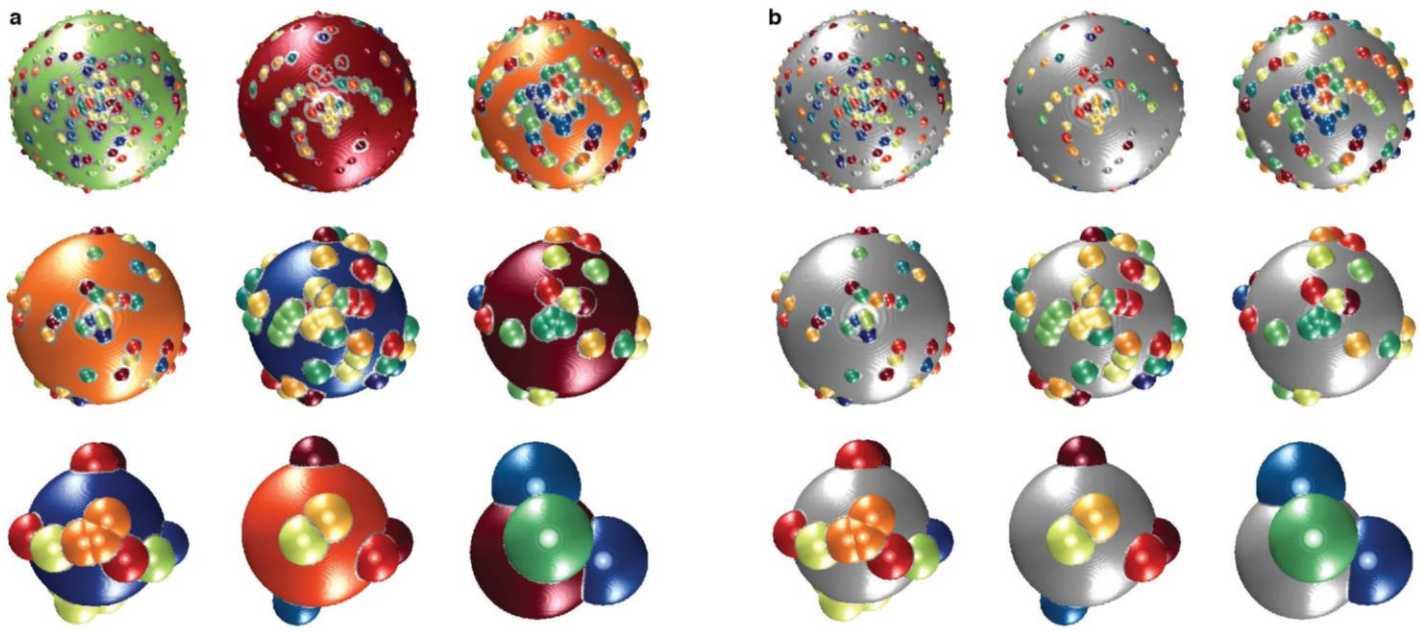

Supplementary Figure 15

Analysis of synthetic images of blebby cells.

(**a**) Segmentation of the cell surface into convex patches via the same workflow used for microscopic data. (**b**) Detection of blebs using a single SVM bleb classifier trained on synthetic data.

	Patch Classification Measures
1	patch volume
2	patch surface area
3	patch perimeter
4	patch radius
5	patch closure surface area
6	patch volume / (patch closure surface area)$^{3/2}$
7	patch surface area / patch closure surface area
8	patch radius / (patch surface area)$^{1/2}$
9	patch surface area / (patch perimeter)^{2}
10	patch variation from a sphere
11	patch shape diameter function
12	maximum mean curvature on patch
13	average of mean curvature on patch
14	standard deviation of mean curvature on patch
15	average Gaussian curvature on patch
16	average of mean curvature on patch edge
17	|patch closure center − average patch position|
18	|weighted average patch position − average patch position| / patch radius
19	|patch closure center − average patch position| / patch radius
20	|patch closure center − weighted average patch position| / patch radius
21	cell volume
22	cell surface area
23	patch count

Supplementary Table 1

Geometric patch features used for SVM-based patch classification.

	Patch Merging Measures
1	average of the mean curvature at the interface between the two patches
2	average of the Gaussian curvature at the interface
3	average of the mean curvature at the interface − the average curvature of the two patches
4	maximum of the mean curvature at the interface
5	maximum of the mean curvature at the interface − the maximum curvature of the two patches
6	standard deviation of the mean curvature at the interface
7	standard deviation of the Gaussian curvature at the interface
8	fraction of mean curvature at the interface that is above 80th percentile for the cell
9	fraction of mean curvature at the interface that is below 20th percentile for the cell
10	fraction of mean curvature at the interface that is above 80th percentile for the two patches
11	fraction of mean curvature at the interface that is below 20th percentile for the two patches
12	fraction of Gaussian curvature at the interface that is above 80th percentile for the cell
13	fraction of Gaussian curvature at the interface that is below 20th percentile for the cell
14	fraction of Gaussian curvature at the interface that is above 80th percentile for the two patches
15	fraction of Gaussian curvature at the interface that is below 20th percentile for the two patches
16	fraction of mean curvature at the interface that is above 90th percentile for the cell
17	fraction of mean curvature at the interface that is below 10th percentile for the cell
18	twice interface length / (perimeter patch 1 + perimeter patch 2)
19	difference in the averages of the mean curvature for the two patches
20	difference in the maxima of the mean curvature for the two patches
21	difference in the (patch closure surface area) / (patch perimeter)^2 for the two patches
22	difference in the (patch volume) / (patch surface area)$^{1.5}$ for the two patches
23	difference in the (patch volume) / (patch closure surface area)$^{1.5}$ for the two patches
24	average of the averages of the mean curvature for the two patches
25	average of the maxima of the mean curvature for the two patches
26	average of the (patch closure surface area) / (patch perimeter)^2 for the two patches
27	average of the (patch volume) / (patch surface area)$^{1.5}$ for the two patches
28	average of the (patch volume) / (patch closure surface area)$^{1.5}$ for the two patches
29	fraction of the interface that is ridged
30	fraction of the interface that is very ridged
31	fraction of the interface that is valley-like
32	fraction of the interface that is very valley-like
33	fraction of the interface that is domed
34	fraction of the interface that is cratered
35	fraction of the interface that is flat
36	fraction of the interface that is saddle-like

Supplementary Table 2

Geometric features of adjacent patch pairs used for SVM-based patch merging.

Distinguishing Features

Blebs vs. Non-Blebs

1 patch volume / (patch closure surface area)$^{3/2}$
2 average of mean curvature on patch edge

Filopodia vs. Non-Filopodia

1 |patch closure center − average patch position|
2 patch surface area
3 |weighted average patch position − average patch position| / patch radius
4 patch surface area / patch closure surface area
5 cell volume
6 average of mean curvature on patch edge
7 patch perimeter

Lamellipodia vs. Non-Lamellipodia

1 |patch closure center − average patch position|
2 patch volume
3 |weighted average patch position − average patch position| / patch radius
4 patch radius / (patch surface area)$^{1/2}$

Supplementary Table 3

Geometric patch features that best distinguish morphological motifs from non-motifs.

	Feature Selection Iterations	Precision	Recall	F_1
Linear SVM	0	0.904	0.965	0.934
Linear SVM	1	0.917	0.955	0.936
Linear SVM	10	0.913	0.960	0.936
Radial SVM	1	0.924	0.874	0.898
Radial SVM	10	0.926	0.949	0.937
Random forest, 30 trees	0	0.950	0.938	0.944
Random forest, 300 trees	0	0.949	0.939	0.944
Random forest, 30 trees	1	0.950	0.938	0.944
Random forest, 30 trees	10	0.954	0.925	0.939

Supplementary Table 4

The precision, recall, and F_1 score of various machine-learning models used for filopodia detection on 13 HBEC cells.

Dataset				Deconvolution parameters			Surface extraction parameters						
								mode *one* parameters			mode *two* parameters		
cell	**label**	**scope**	**motif**	**mode**	**param.**	**apo. height**	**mode**	**image smooth**	**image gamma**	**mesh smooth**	**inside gamma**	**dilate radius**	**erode radius**
dendritic	Lifeact	meSPIM	lamellipodia	Wiener	0.018	0.06	three	0	1	6	0.6	5	6.5
melanoma	tractin	meSPIM	blebs	Wiener	0.018	0.04	one	0	1	0			
HBEC	tractin	meSPIM	filopodia	Wiener	0.015	0	one	0.6	1	0			
melanoma	Kras	meSPIM	blebs	Wiener	0.018	0.06	one	0	0.7	0			
melanoma	PIP_2	meSPIM	blebs	Wiener	0.018	0.06	two	0	0.7	0	0.6	4	6
melanoma	tractin	meSPIM	blebs & filopodia	Wiener	0.015	0	one	0.6	1	2			
melanoma	tractin	meSPIM	filopodia	Wiener	0.015	0	one	0.6	1	2			
U2OS	tractin	meSPIM	blebs	RL	8	0.08	two	0	0.5	0	0.6	5	6
melanoma	PI3K	ASLM	blebs	RL	7	0.06	two	0	0.7	0	0.6	4	6
melanoma	tractin	confocal	blebs	RL	10	0	two	1	0.6	6	0.6	5	6
microglia	P2Y12	light sheet	extensions	RL	10	0.06	three	0	1	6	0.5	5	6.5
melanoma	cytosol	ASLM	blebs	RL	10	0.04	one	0	1	6			
T cell	Lifeact	lattice	lamellipodia	RL	10	0.06	three	0	0.8	6	0.3	5	6
breast cancer	CAAX	AO lattice	extensions	none			one	0.8	0.45	30			
melanoma	cytosol & tractin	meSPIM	blebs	Wiener	auto	0.055	one	0	1	0			
melanoma	cytosol	meSPIM	blebs	Wiener	auto	0.04	one	0	1	0			

Supplementary Table 5

Deconvolution and surface extraction parameters for all described datasets.

In the deconvolution parameters section, RL refers to Richardson-Lucy deconvolution. For Wiener deconvolution, the *param* column shows the Wiener parameter, whereas for Richardson-Lucy deconvolution it shows the number of iterations. In the surface extraction parameters section, in mode *one* an isosurface is created directly from the Otsu-normalized deconvolved image, in mode *two*, it is created from the combination of the Otsu-normalized image and an “inside” image, and in mode *three*, it is created from the combination of the Otsu-normalized image, an “inside” image, and a surface filtered image.

Features Selected

User 1
patch radius / (patch surface area)$^{1/2}$
average of mean curvature on patch edge
patch shape diameter function
|patch closure center − average patch position|
|weighted average patch position − average patch position| / patch radius
|patch closure center − average patch position| / patch radius
|patch closure center − weighted average patch position| / patch radius
cell volume
cell surface area

User 2
patch closure surface area
patch volume / (patch closure surface area)$^{3/2}$
patch surface area / (patch perimeter)^{2}
patch shape diameter function
average of mean curvature on patch
average of mean curvature on patch edge

User 3
patch closure surface area
patch radius / (patch surface area)$^{1/2}$
maximum mean curvature on patch
|patch closure center − average patch position|

Supplementary Table 6

Automatically selected features for bleb detection models generated from three different users training on the same four cells.